

# Response of Ductile Metal Sheet Parameters to the Cone Angle of Indenting Conical Tool and Fracture Toughness Evaluation

Malik M. Nazeer, M. Afzal Khan, A. Naeem, and A.-ul Haq

(Submitted 3 May 1999; in revised form 25 June 2000)

The indentation and perforation of ductile metal sheet with a conical tool is accompanied by elastoplastic bending, stretching, plastic flow, and crack initiation and propagation. This ultimately results in material fracture in the form of petals. It has been observed that the perforation process is dependent upon the angle of the conical tool. Fracture toughness, crack initiation, work input before and after crack initiation, number of petals, and sheet and petal bending angles all depend on the tool angle. Crack initiation has resulted at minimum tool displacement for a tool angle  $\alpha = 45^\circ$ , while minimum work input before and after the crack initiation is observed when the tool has an angle  $\alpha = 35^\circ$ . The optimum range of tool angles for the indentation process is  $\alpha = 22.5$  to  $50^\circ$ . In this range, the aluminum sheets showed minimum fracture toughness as well as minimum work input to overcome the offered resistance.

**Keywords** crack initiation, ductile metal sheet, fracture toughness

## 1. Introduction

Perforation and petal formation is the result of complicated modes of deformation due to plastic bending, stretching, and crack propagation. It depends on the metal properties, tool angle, sheet thickness, and speed of indentation and sample size (inside holding die).<sup>[1]</sup> The particular deformation range (when fracture does occur) depends on both size and geometry of the tool, and on the specimen material, as a generalized body (shape) will behave differently depending on the material characteristics.<sup>[2]</sup> The process of conical tool indentation was studied and mathematically analyzed in Ref 3, while in Ref 4, it was upgraded with the help of numerical techniques for better understanding of different parameter response. Based upon this analysis and the computer code developed in Ref 3 and 4, the response of different parameters to sheet thickness was presented in Ref 5, whereas study of various parameter responses to the tool angle variation is presented and discussed in the present work.

## 2. Experimental Procedures

The conical tool indenting tests were carried out with the help of the Instron universal testing machine (Kahuta, Pakistan) (model 4302) using conical tools of angles ( $2\alpha =$ ) 20, 45, 70, 90, 100, and  $120^\circ$ . For these experiments, specimens of 90 mm diameter were cut in a manual screw press from SIC half-hard and NS4 aluminum alloy sheets of various thicknesses. The

material percentage composition of SIC (approximately AA1100) samples was Fe, Si, Mg, Mn, Zn, and Cu at 0.2, 0.3, 0.1, 0.1, 0.1, and 0.1, respectively (the balance was aluminum), whereas that of NS4 (approximately AA5052) was Fe, Si, Mg, Mn, Zn, and Cu at 0.5, 0.5, 1.7 to 2.4, 0.5, 0.25, and 0.25, respectively (the balance was aluminum). The tests with all the tools were carried out on a SIC half-hard, 22 gauge (0.66 mm) thick sheet, whereas for other thicknesses of SIC and NS4 material, only three tools with angle  $\alpha = 10, 35,$  and  $60^\circ$  were used just for verification of the results. The corresponding load versus displacement data were plotted with an  $(x, y)$  chart recorder. A computer program developed on the basis of Ref 4 has been used to obtain the results.

## 3. Results and Discussion

The results for the conical tool indentation tests in SIC half-hard aluminum sheets of 0.66, 0.90, 1.20, and 1.50 mm thicknesses and that of NS4 of 0.56, 0.90, and 1.20 mm thicknesses are plotted in Fig. 1 through 8. The response of different parameters to the angle of the indenting conical tool are presented and discussed in the following sections.

### 3.1 Load Displacement

Figure 1 shows the behavior of a load versus tool displacement curve for different tool angles. In the pure elastic bending zone, all the curves are linear as well as collinear with each other, showing that slope of elastic bending curves is independent of tool angle. However, the separate departure of each load versus tool displacement curve at the end of this pure elastic bending zone, where plastic flow intermixing with elastic deformations begins, is dependent on tool angle. The pure elastic bending limit increases with the tool angle. For equal displacement, the load increases slowly below tool angle  $\alpha = 35^\circ$ , whereas it increases abruptly beyond this. However, the displacement decreases with the decreasing tool angle above  $\alpha = 35^\circ$ , whereas

Malik M. Nazeer, M. Afzal Khan, A. Naeem, and A.-ul Haq, Dr. A.Q. Khan Research Laboratories, Rawalpindi, Pakistan. Contact e-mail: mmnazeer@inst-rd.isb.sdnpc.org.

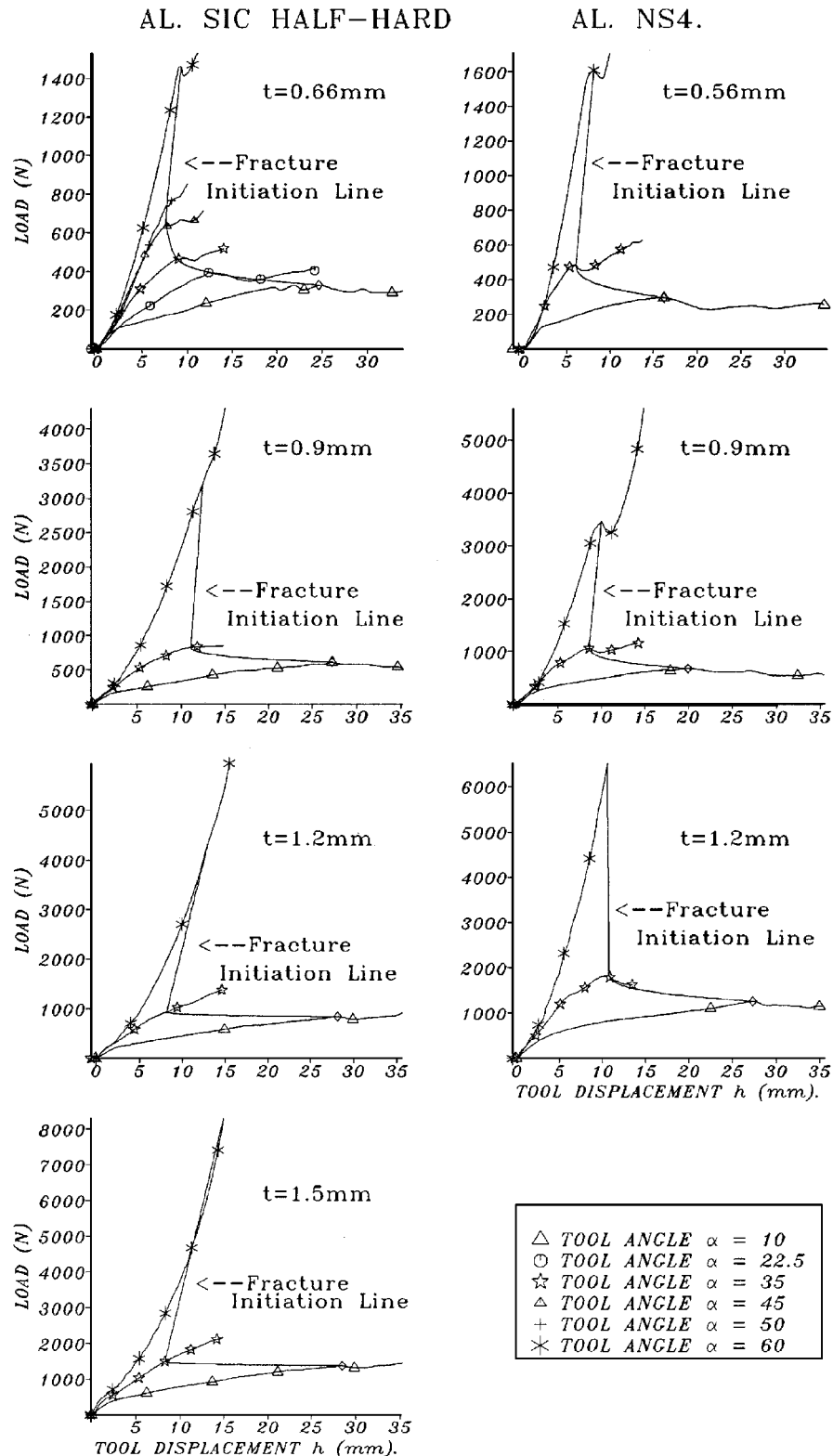


**Fig. 1** Load versus tool displacement

it increases abruptly below this angle. This figure also confirms that the above observations are also true for other thicknesses as well as NS4 and, hence, other ductile materials.

### 3.2 Crack Initiation

Figure 1 also shows a line crossing each load-displacement curve, through the crack initiation points. The load required

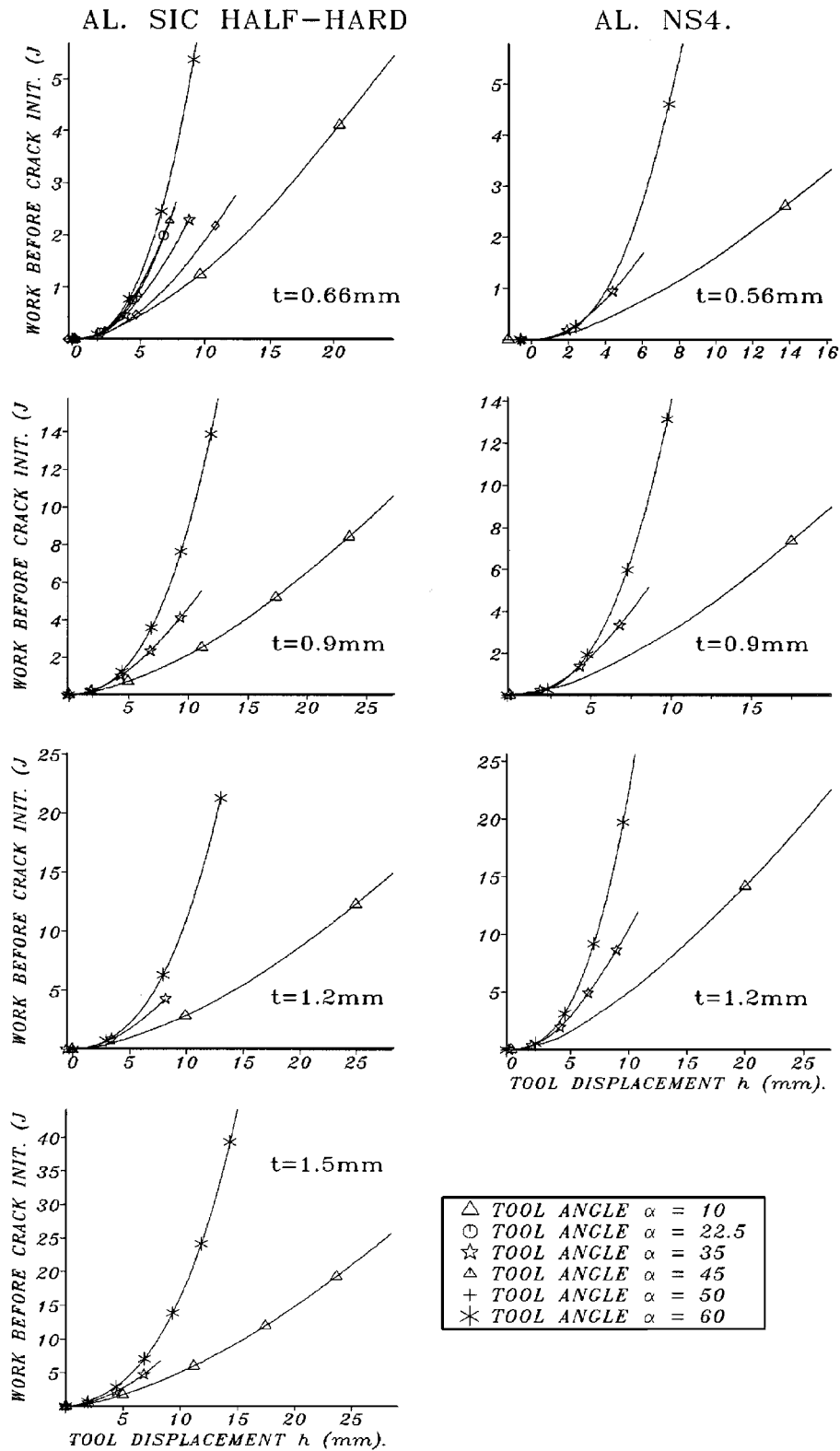


**Fig. 2** Work input before crack initiation versus tool displacement

for crack initiation increases asymptotically with the tool angle  $\alpha$  above  $35^\circ$ , whereas crack initiation displacement increases asymptotically with the decrease in tool angle  $\alpha$  below  $35^\circ$ .

The drop in load at the crack initiation point and change in the load-displacement curve path and pattern beyond this point are clearly visible. The pattern of curves for other sheet thicknesses

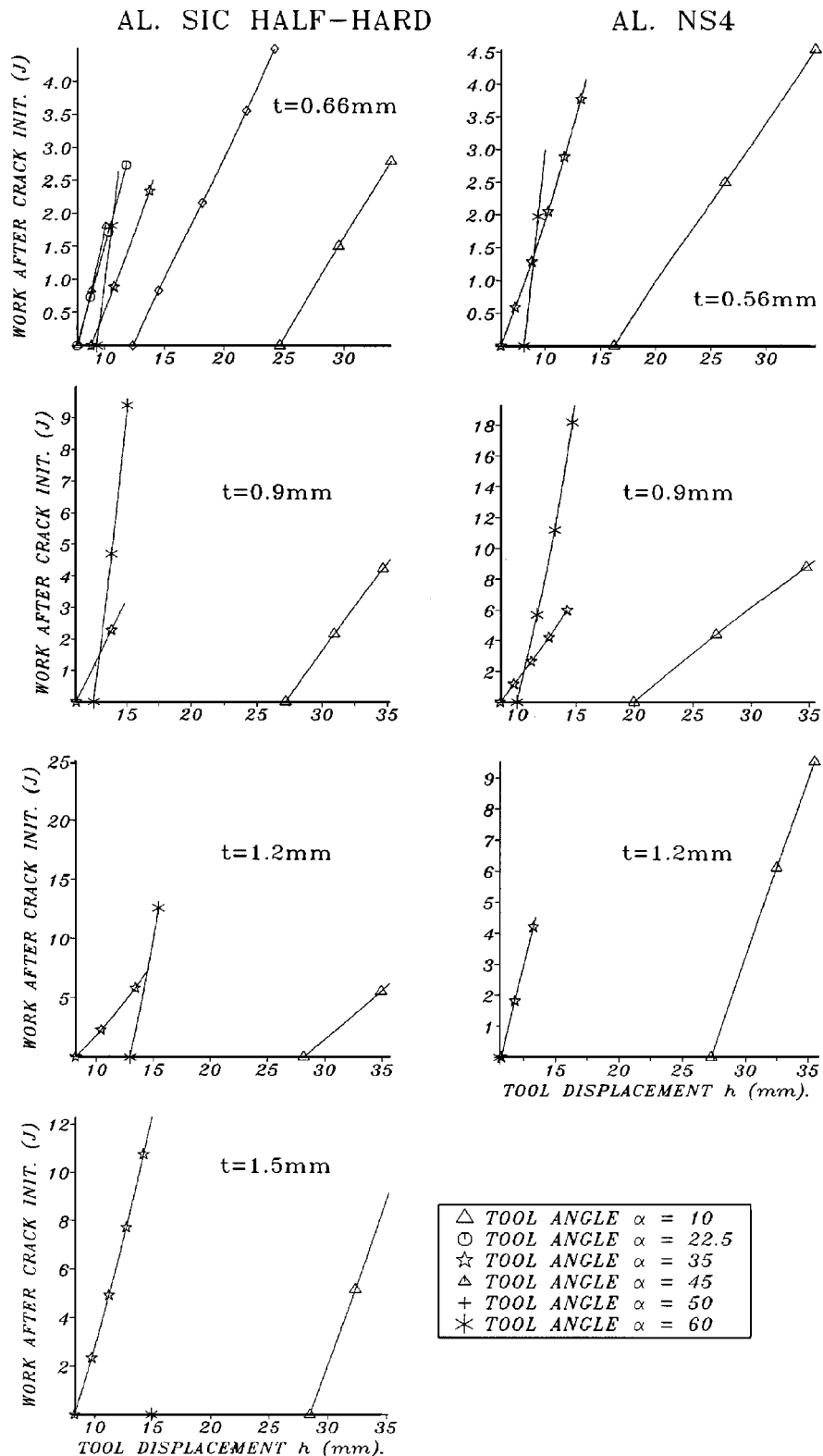


Fig. 3 Work input after crack initiation versus tool displacement

of SIC half-hard and NS4 material show the versatility of the above observations with sheet thickness and material.

### 3.3 Work Input before Crack Initiation

Figure 2 shows work input before crack initiation versus tool displacement  $h$ . Initially, the work input is linear as well

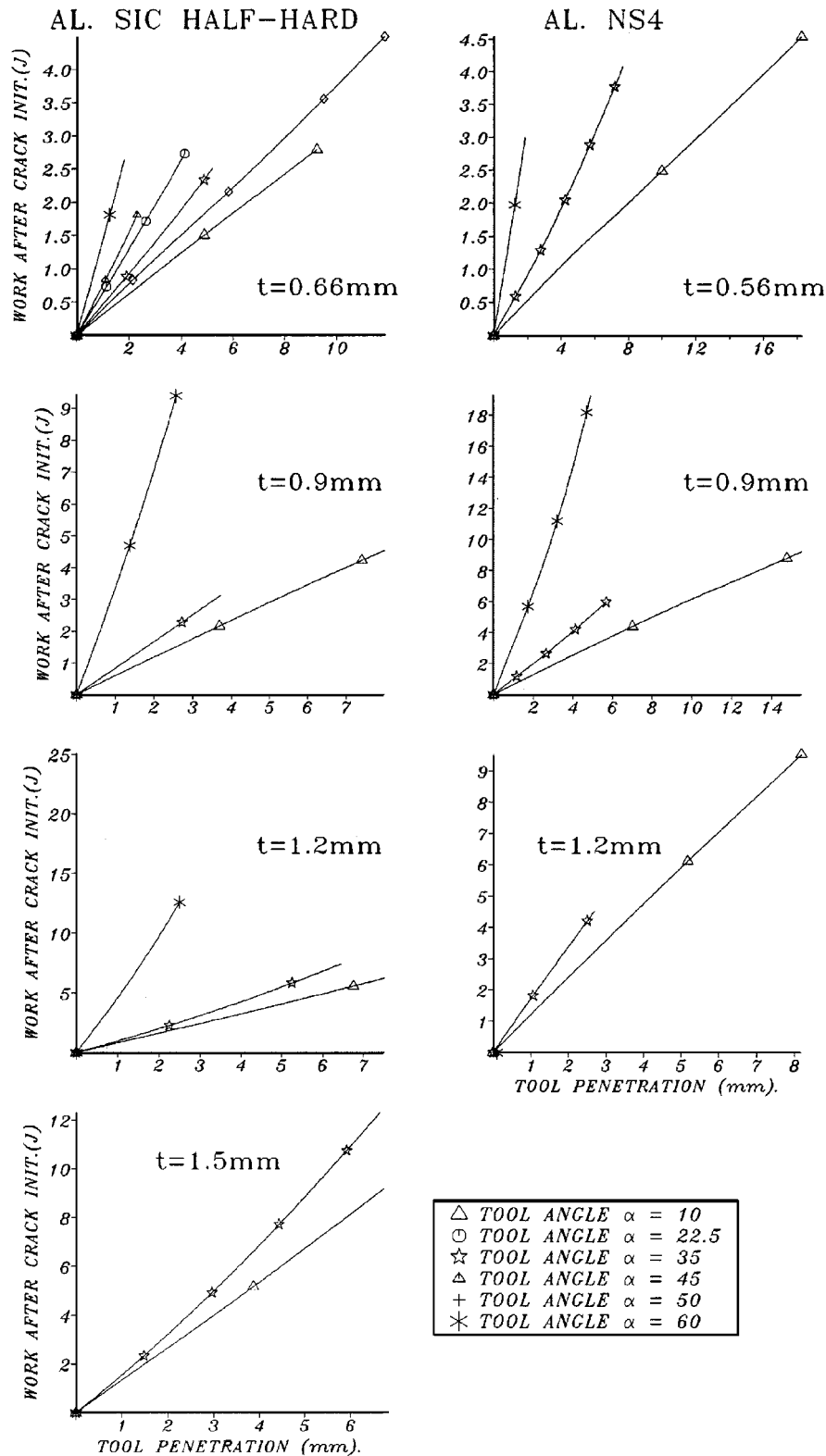
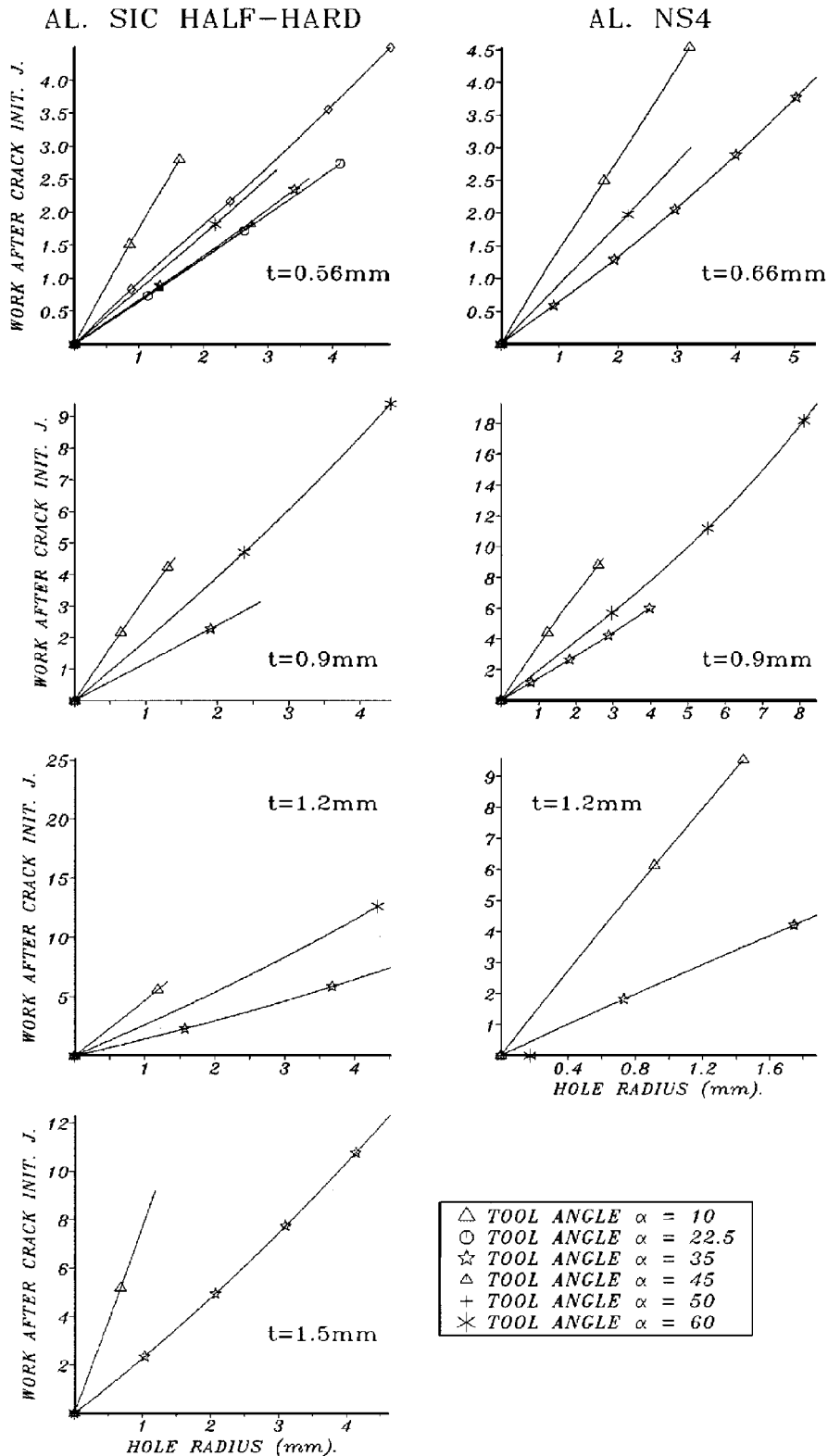


Fig. 4 Work input after crack initiation versus tool penetration

as mutually collinear in the pure elastic bending zone, showing its independence of tool angle in this range. Then it becomes nonlinear in the combined elastic and plastic bending range with

the lines departing from each other, showing its dependence on the tool angle. After the end of elastic bending, it again becomes linear, but with different slopes for different tool angles, show-



**Fig. 5** Work input after crack initiation versus hole diameter

ing its dependence on tool angle. The slope of the curves increases with the tool angle, which means that the rate of work input increases with the tool angle. The terminal ends of these

curves point to the total work input up to the crack initiation point. The tool with  $\alpha = 35^\circ$  shows minimum work input for crack initiation. The other sets of curves confirm the above

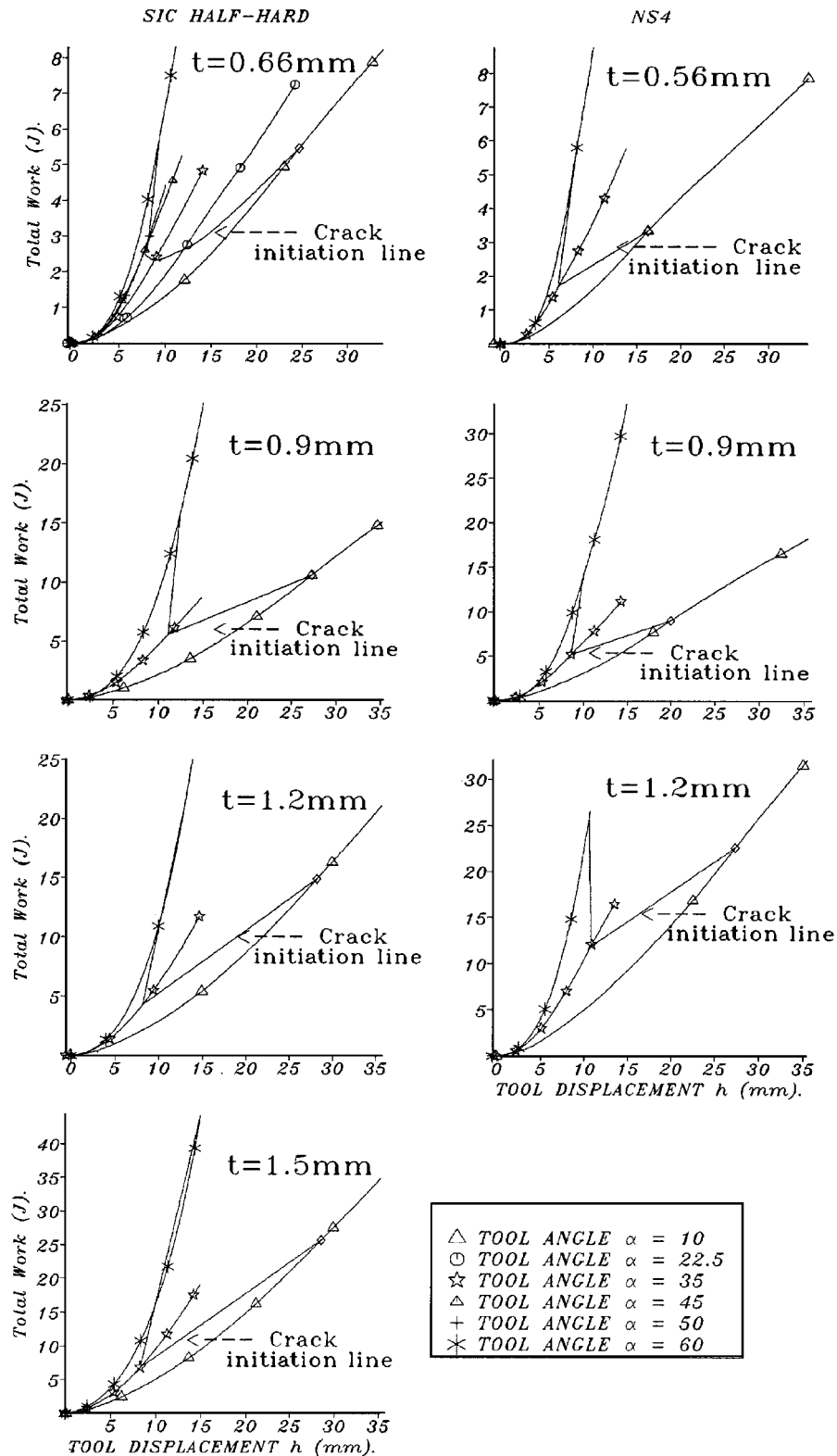


**Fig. 6** Total work input versus tool angle

findings for other sheet thicknesses of SIC half-hard and NS4 materials.

### 3.4 Work Input after Crack Initiation

Figure 3 shows linearity of work input after crack initiation versus conical tool displacement. The rate of work input

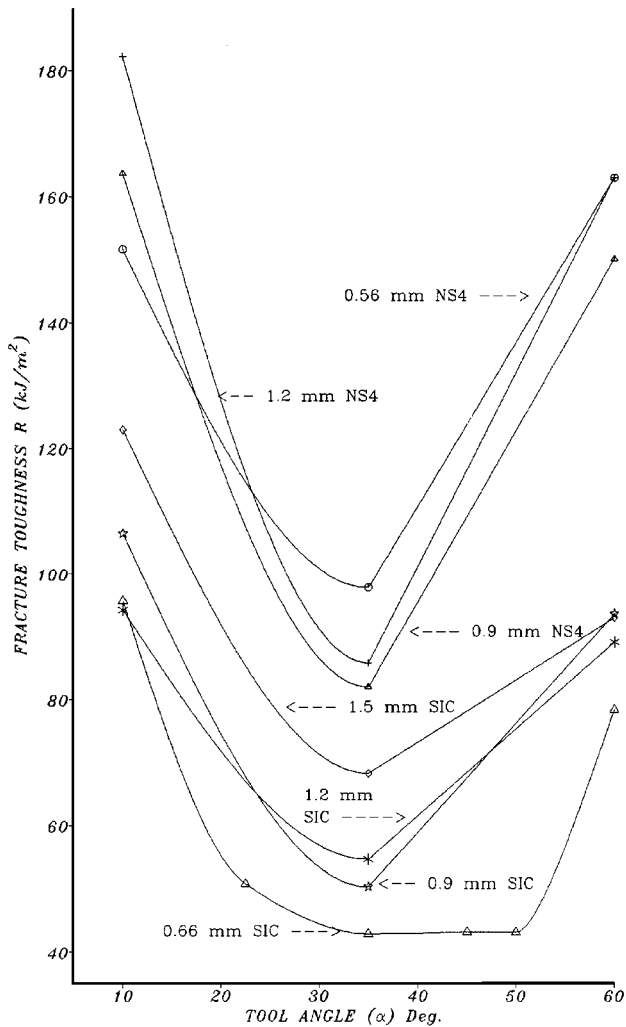


Fig. 7 Fracture toughness versus tool angle

increases with the tool angle. The minimum displacement at crack initiation for  $\alpha = 45^\circ$  is also clearly visible. The above finding of increase in work input rate with the tool angle is clearer in Fig. 4, where work input after crack initiation is plotted versus tool penetration after crack initiation for different sheet thicknesses. It also confirms this finding for other sheet thicknesses of SIC and NS4 materials. In Fig. 5, this work is plotted versus radius of the hole developed, and it shows that the tools with angle  $\alpha = 35$  to  $50^\circ$  are most suitable for tool penetration. The tool with angle  $\alpha = 35^\circ$  is the best, with minimum slope, whereas that with  $\alpha = 10^\circ$  is the most awkward. The sets of curves for other sheet thicknesses of SIC and NS4 materials in Fig. 3 through 5 verify the above findings with respect to sheet thickness and materials.

### 3.5 Total Work

Figure 6 shows total work input versus tool displacement, along with a line passing through the crack initiation point on each curve. The status of these curves before and after the crack

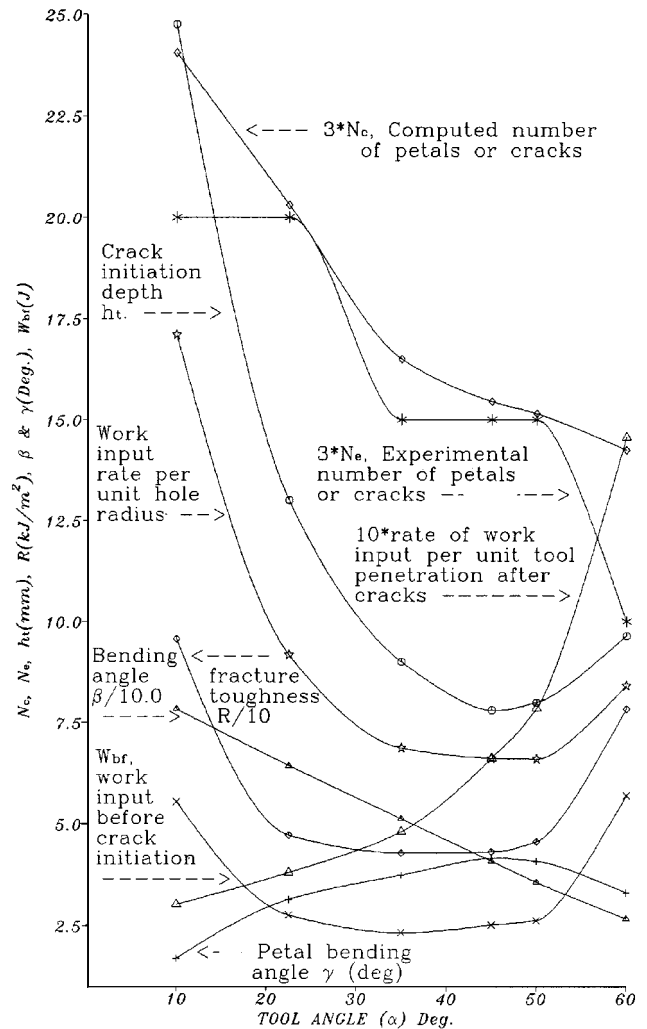


Fig. 8 Different parameters versus tool angle

initiation point is already discussed in Fig. 2 through 5. Here it is worth noting that work input before and after the crack initiation point is linear, with the same constant slope showing that rate of work input does not change with penetration of tool or crack initiation, contrary to the case of ball indentation,<sup>[1,6]</sup> where it decreases after crack initiation. This also shows that the rate of work input increases with the tool angle, and findings related in the discussion of Fig. 3 through 5 for the case after crack initiation are also true for the case before the crack initiation point, as far as pure plastic bending is concerned. The elastic deformation and elastic work input rate being independent of tool angle, the above findings of tool dependence are also true for the transition or mixed range. Figure 6 also confirms the generality of these findings with respect to sheet thickness and ductile materials.

### 3.6 Fracture Toughness

Figure 7 shows the evaluated fracture toughness versus tool angle for both SIC half-hard and NS4 aluminum sheets. These



curves show the material and sheet thickness response to the tool angle variation along with their mutual comparison. The similar dependence of fracture toughness to the tool angle is clear from all the curves showing optimum tool angle of  $\alpha = 35^\circ$ . The minute increase of fracture toughness with the sheet thickness is also clear from this figure, both for SIC and NS4 sheets. This confirms that a tool with  $\alpha = 35^\circ$  is the best or optimum one, requiring minimum work input for crack initiation and tool penetration.

### 3.7 Overall Response of 0.66 mm SIC Sheet

Figure 8 shows the overall response of various parameters of 0.66 mm SIC half-hard aluminum sheet to tool angle variation. The computed numbers of petals (without rounding),  $n_c$ , decreases linearly with the increase in tool angle, but has a turning point at tool angle  $\alpha = 35^\circ$ . The rate of decrease is large before  $\alpha = 35^\circ$  and smaller after this. The curve for the experimental number of petals is in steps because of rounding of the fractions; however, this too has a turning point at  $\alpha = 35^\circ$ . The curve for displacement at crack initiation points is smooth and regular. Initially, it decreases with the increase in tool angle with a decreasing rate until  $\alpha = 45^\circ$ , and then starts increasing with increasing rate. The crack initiation displacement is minimum for  $\alpha = 45^\circ$ . This behavior of conical tool to the crack initiation is contrary to the process of ball indentation, where the smaller the diameter of the ball, the smaller is the displacement before crack initiation.<sup>[1,3,6]</sup> The sheet-bending angle  $\beta$  decreases almost linearly with the increase in tool angle. The petal-bending angle  $\chi$  increases with the increasing tool angle until  $\alpha = 45^\circ$ . Thereafter it starts decreasing, showing maximum value for  $\alpha = 45^\circ$ .

The work input before crack initiation and fracture toughness curves shows similar but interesting behavior. They both decrease sharply with the increase in tool angle until  $\alpha = 22.5^\circ$ , thereafter, they both decrease minutely with minimum value at  $\alpha = 35^\circ$  and then increase minutely until  $\alpha = 50^\circ$  and then increase sharply. This shows that the optimum value of  $\alpha$  is  $35^\circ$ , with the most suitable range of tool angle  $\alpha$  being between  $22.5$  and  $50^\circ$ , and beyond these limits, the tool is worthless. This also shows that the fracture toughness of the material is dependent on conical tool angle. The SIC half-hard aluminum sheet of 0.66 mm can easily be fractured with a conical tool of angle  $\alpha$  between  $22.5$  and  $50^\circ$ , and this also holds for other sheet thicknesses and other ductile materials, as is evident from the above discussion.

The rate of work input per unit radius of the generated hole after crack initiation decreases with the tool angle at a decreasing rate with the minimum at  $\alpha = 50^\circ$ , and then increases at an increasing rate. The optimum range of tool angle is between  $\alpha = 35$  and  $50^\circ$ . The rate of work input per unit tool penetration after crack initiation increases linearly with the tool angle until  $\alpha = 35^\circ$ , where it increases nonlinearly until  $\alpha = 50^\circ$ , and thereafter increases linearly at a higher rate. This also shows that the optimum range of tool angle is between  $\alpha = 35$  to  $50^\circ$ . This also holds good for work before crack initiation because the rate of work input does not change at the crack initiation, as stated above in the discussion of Figure 6.

## 4. Conclusions

From the above discussion, the following conclusions were obtained.

- The fracture toughness analysis of sheets of different thicknesses of this and other ductile materials can be performed by indentation and perforation with conical tool.
- The sheet bending angle  $\beta$  decreases almost linearly with the change of conical tool angle.
- The number of petals decreases linearly with the change of conical tool angle, but at two different rates. The rate of decrease in petal number is larger above  $\alpha = 35^\circ$  than below this with a sharp turn at  $\alpha = 35^\circ$ .
- The displacement of the tool at crack initiation decreases regularly at a decreasing rate with minimum displacement for  $\alpha = 45^\circ$  and thereafter increases at an increasing rate.
- The petal bending angle  $\gamma$  increases regularly at a decreasing rate with a maximum at  $\alpha = 45^\circ$  and thereafter decreases at an increasing rate.
- The fracture toughness depends on tool angle. It decreases sharply until  $\alpha = 22.5^\circ$  and then decreases slowly, with a minimum at  $\alpha = 35^\circ$ . Thereafter, it increases slowly until  $\alpha = 50^\circ$ , and then increases sharply.
- The results are reproducible in the ductile metal sheets.
- The mathematical analysis of rigid-plastic fracture mechanics and the computer code developed can be used to find the number of cracks/petals formed and the fracture toughness of the material. The ductile metal sheet offers minimum resistance to the conical tool with  $\alpha = 35^\circ$  with a suitable range of  $\alpha = 22.5$  to  $50^\circ$ . This may be the best range for nose angle of offensive armors such as antitank and vessel missiles, rockets, and other projectiles.
- The optimal trend of the response of ductile metal sheet parameters to the indenting conical tool is a characteristic of a conical tool and has not been observed in sharp tool<sup>[7,8]</sup> and ball<sup>[1,9]</sup> indentation.

## Acknowledgments

The authors are thankful to Professor A.G. Atkins for his guidance in this work. Thanks are also due to Mr. Khalid Kamal for his help in drawing the graphs.

## References

1. M. Afzal Khan, M.M. Nazeer, Athar Naeem, A.-ul Haq, and A. G. Atkins: *Proc. Eur Conf. Advanced Materials and Processes [EURO-MAT 95], Symp. D*, Padua/Venice, Italy, Associazione Italiana di Metallurgia, 1-20121 Milano Piazzale Rodolfo Morandi, 2, 1995, pp. 491-94.
2. A.G. Atkins: *Future Trends in Applied Mechanics* (P.S. Theocaris Festschrift), National Technical University of Athens, Athens, 1989.
3. M. Afzal Khan: Ph.D. Thesis, Reading University, Reading, United Kingdom, 1996, pp. 262-341.
4. Malik M. Nazeer, M. Afzal Khan, Athar Naeem, and A.-ul Haq: *Int. J. Mech. Sci.*, 2000, vol. 42, pp. 1391-1403.

5. Malik M. Nazeer, Athar Naeem, M. Afzal Khan, A.-ul Haq, and A.G. Atkins: *Proc. 5th Int. Symp. Advanced Materials*, Islamabad, Pakistan, M. Afzal Khan, A.-ul Haq, K. Hussain, and A.Q. Khan, eds., Dr. A.Q. Khan Research Laboratories, Kahuta, Pakistan, 1997, pp. 552-59.
6. Malik M. Nazeer, Athar Naeem, M. Afzal Khan, A.-ul Haq, and A.G. Atkins: *Proc. 12th Nat. Conf. Engineering Fracture Mechanics*, Jamshoro, Pakistan, 1997.
7. M. Afzal Khan, Athar Naeem, Malik M. Nazeer, A.-ul Haq, and A.G. Atkins: *Proc. 3rd Int. Symp. Advanced Materials*, Islamabad, Pakistan, A.-ul Haq, F. Habiby, and A.Q. Khan, eds., Dr. A.Q. Khan Research Laboratories, Kahuta, Pakistan, 1993, pp. 706-13.
8. Malik M. Nazeer, M. Afzal Khan, Athar Naeem, A.-ul Haq, and A.G. Atkins: *Proc. Int. Conf. Applied and Pure Mathematics, ICPAM 95*, Bahrain, Bahrain University, Bahrain, in press.
9. A.G. Atkins, M. Afzal Khan, and J.M. Liu: *Int. J. Impact Eng.*, 1998, vol. 21 (7), pp. 521-39.